Supporting Information

Standards and Protocols for Data Acquisition and Reporting for Studies of the Electrochemical Reduction of Carbon Dioxide

Ezra L. Clark[† 1,2], Joaquin Resasco[† 1,2], Alan Landers[3,5], John Lin[4,5], Linh-Thao Chung,[2] Amber Walton,[2] Christopher Hahn[4,5], Thomas F. Jaramillo[4,5], Alexis T. Bell[1,2]*

† These authors contributed equally to this work

1. Joint Center for Artificial Photosynthesis
Lawrence Berkeley National Laboratory
Berkeley, CA 94720

2. Department of Chemical and Biomolecular Engineering
University of California
Berkeley, CA 94720

3. Department of Chemistry
Stanford University
Stanford, CA 94305

4. Department of Chemical Engineering
Stanford University
Stanford, CA 94305

5. SUNCAT Center for Interface Science and Catalysis
Stanford University, Stanford, CA 94305
SLAC National Accelerator Laboratory
Menlo Park, CA 91125

Submitted to

ACS Catalysis

*To whom correspondence should be sent: alexbell@berkeley.edu

Supporting Information

Table of Contents

Supporting Information

SI-1: Experimental Methods at the University of California at Berkeley

Electrode Preparation

Epitaxial Cu and Ag thin films were prepared by sputter disposition onto single-side polished Si(111), (100), or (110) wafers (Virginia semiconductor, 1-10 Ω cm). The native oxide was removed from the surface of the Si substrates prior to deposition by submerging them in a 10 wt. % HF solution for 5 min. Immediately after HF etching the Si wafers were transferred into an AJA ATC Orion-5 sputtering system for deposition. The Cu (99.999% Kurt Lesker) and Ag (99.999% Kurt Lesker) were deposited under Ar at a pressure of 2 mTorr at a rate of 1 Å/s, which was calibrated using a quartz crystal monitor. The total film thickness deposited was 100 nm. Cu deposition was conducted at ambient temperature whereas Ag deposition was conducted at 300 °C by heating the sample stage using an IR lamp. Cu(111) and (100) oriented thin films were obtained by deposition onto Si(110) and (100) substrates, respectively, whereas Ag(111) and (100) oriented thin films were obtained by deposition onto Si(111) and (100) substrates, respectively. Ag foils (99.999% Alfa Aesar) were mechanically polished with a series of sandpapers (600, 1200, and 2500 grit 3M) and sonicated in DI water for 30 min before electrochemical testing.

Electrode Characterization

The structure of the Cu and Ag thin films were characterized by X-ray diffraction. The orientation and epitaxial quality of the films were determined using symmetric θ-2θ scans, in plane ϕ scans, ω scans or rocking curves, and pole figures. XRD patterns were taken with a PANanalytical X'Pert diffractometer using Cu Kα radiation (λ = 1.54056 Å). Symmetric θ-2θ scans were collected on samples fixed onto a flat glass slide in locked-coupled mode with a goniometer resolution of 0.001°. The near-surface composition of electrodes was measured using

a Kratos Axis Ultra DLD X-ray photoelectron spectrometer (XPS). All spectra were acquired using monochromatized Al Kα radiation (15 kV, 15 mA). Ar sputtering of the sample surface was avoided to prevent surface composition changes. The kinetic energy scale of the measured core level spectra was calibrated by setting the C 1s binding energy to 284.8 eV. Further analysis of surface composition was done using low energy ion scattering spectroscopy (LEIS) using the same instrument. All LEIS spectra were acquired using a focused He ion beam (1 kV).

Electrochemical Measurements

All electrochemical experiments were conducted in a gas-tight electrochemical cell machined from polyether ether ketone (PEEK). A schematic of the cell is shown below in Figure S1. Further details of this electrochemical cell are described in previous works.[1] The cell was sonicated in 20 wt. % nitric acid and thoroughly rinsed with DI water prior to all experimentation. The working and counter electrodes were parallel and separated by an anion-conducting membrane (Selemion AMV AGC Inc.). Gas dispersion frits were incorporated into both electrode chambers to provide ample electrolyte mixing. The exposed geometric surface area of each electrode was 1 cm^2 and the electrolyte volume of each electrode chamber was 1.8 mL. The counter electrode was a glassy carbon plate (Type 2 Alfa Aesar) that was also sonicated in 20 wt. % nitric acid prior to all experimentation. Platinum foil was also used as the anode. The working electrode potential was referenced against a Ag/AgCl electrode (Innovative Instruments Inc.) that was calibrated against a homemade standard hydrogen electrode. A 0.05 M M_2CO_3 (99.995% Sigma Aldrich) solution prepared using 18.2 MΩ DI water was used as the electrolyte. Metallic impurities in the as-prepared electrolyte were removed before electrolysis by chelating the solution with Chelex 100 (Na form Sigma Aldrich). Both electrode chambers were sparged with CO_2 (99.999% Praxair Inc.) at a rate of 2.5 to 40 sccm for 30 min prior to and throughout

the duration of all electrochemical measurements. Upon saturation with CO_2 the pH of the electrolyte was 6.8, which was maintained throughout the duration of chronoamperometry.

Electrochemistry was performed using a Biologic VSP-300 potentiostat. All electrochemical measurements were recorded versus the reference electrode and converted to the RHE scale. Potentiostatic electrochemical impedance spectroscopy (PEIS) was used to determine the uncompensated resistance (R_u) of the electrochemical cell by applying voltage waveforms about the open circuit potential with an amplitude of 20 mV and frequencies ranging from 50 Hz to 500 kHz. The potentiostat compensated for 85% of R_u *in-situ* and the last 15% was post-corrected to arrive at accurate potentials. The electrocatalytic activity of each electrode was assessed by conducting a chronoamperometry staircase at increasingly negative applied potentials.

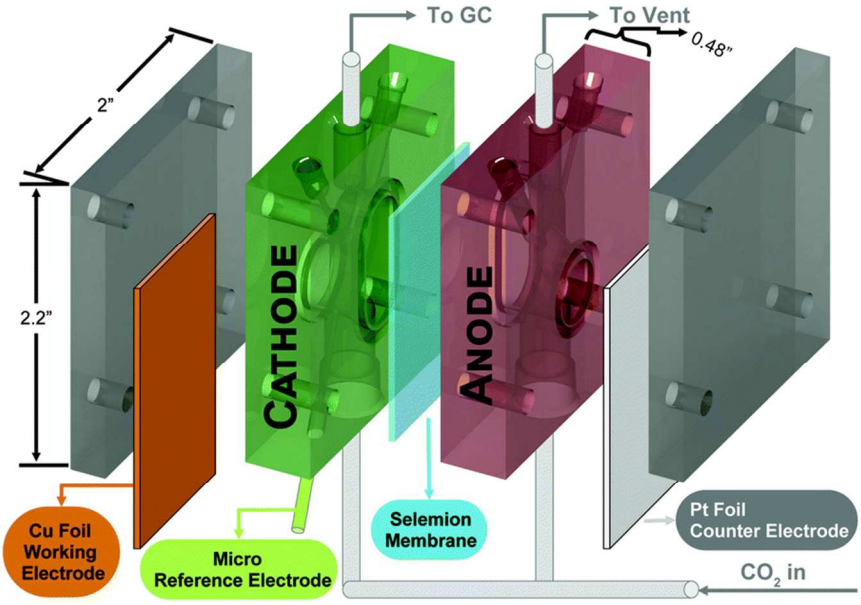

Figure S1: Schematic of the electrochemical cell used for testing. Reproduced from Lobaccaro et al[1]. Copyright 2016, Royal Society of Chemistry.

Product Analysis

The effluent from the electrochemical cell was introduced directly into the sampling loop of an Agilent 7890B gas chromatograph (GC) equipped with a pulsed-discharge helium ionization detector (PDHID). The effluent was sampled after the first 10 min of chronoamperometry and every 14 min

thereafter. The constituents of the gaseous sample were separated in He (99.9999% Praxair Inc.) using a Hayesep-Q capillary column (Agilent) in series with a packed ShinCarbon ST column (Restek Co.). After sampling the reaction effluent the column oven was maintained at 50 °C for 1 min followed by a temperature ramp at 30 °C/min to 250 °C, which was maintained for the duration of the analysis. The signal response of the PDHID was calibrated by analyzing a series of NIST-traceable standard gas mixtures (Airgas Inc.).

The electrolyte from both electrode chambers was collected after electrolysis and analyzed using a Thermo Scientific UltiMate 3000 liquid chromatograph (HPLC) equipped with a refractive index detector (RID). The electrolyte samples were stored in a refrigerated autosampler until analyzed in order to minimize the evaporation of volatile liquid-phase reaction products. The liquid-phase products contained in a 10 μL aliquot were separated using a series of two Aminex HPX 87-H columns (Bio-Rad Inc.) and a 1 mM sulfuric acid eluent (99.999% Sigma Aldrich). The column oven was maintained at 60 °C for the duration of the analysis. The signal response of the RID was calibrated by analyzing standard solutions of each product at a concentration of 1, 10, and 50 mM.

SI-2: Experimental Methods at Stanford University

The experimental methods employed at Stanford University have been fully described in previous works.[2, 3] The electrode preparation and electrochemical testing was conducted using similar methodologies as those employed at the University of California at Berkeley. The electrochemical experiments were conducted in a gas-tight electrochemical cell machined from polycarbonate. A schematic of the cell is shown in Figure S2. Further details of this electrochemical cell are described in previous works.[4] 0.1 M $KHCO_3$ (Sigma-Aldrich, 99.99% metals basis) was used as the electrolyte, which was constantly sparged with CO_2 (5.0, Praxair) at a flow rate of 20 sccm. The pH of the electrolyte was maintained at 6.8 during all experimentation. The effluent of the electrochemical cell was introduced directly into the sampling loop of a gas chromatograph (GC, SRI 8610C in the Multi-Gas #3 configuration). The compartments of the electrochemical cell were separated by an anion exchange membrane (Selemion AMV, AGC Inc.). A Ag/AgCl (Accumet) electrode was used as the reference electrode and a platinum foil was used as the counter electrode. Polycrystalline silver foil (Alfa Aesar, 0.1 mm thickness, 99.998% metals basis), was mechanically polished (3M, 400 grit) and rinsed with water until no discoloration was observed on the surface prior to each electrochemical experiment. Thin films of Cu were prepared inside a Temescal BJD-1800 chamber by electron beam evaporation. Si(100) and (110) were used as substrates to produce epitaxial Cu(100) and (111) thin films, respectively. The native oxide was removed with buffered hydrofluoric acid (BHF) before loading the samples into the chamber. After evacuating the chamber, 100 nm of Cu was deposited at 2 Å/s on the Si substrates.

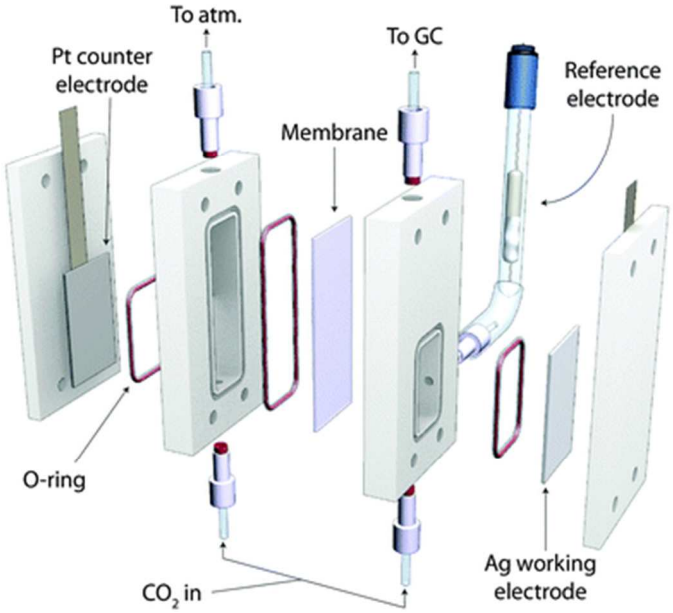

Figure S2: Schematic of the electrochemical cell used for comparison testing (Stanford University). From Hatsukade et al.[2] Copyright 2014, Royal Society of Chemistry.

SI-3: Impact of Mechanical Polishing on Surface Purity

Different surface preparation methods can introduce variations in the activity and selectivity between samples of the same metal.[5, 6] Surface preparation methods reported in the literature include various forms of mechanical and electrochemical polishing. Understanding how these treatments affect the purity of the catalyst surface is critical to obtaining accurate and reproducible results. Figure S3 shows the surface composition of a Cu foil after various mechanical polishing treatments. Residues of the polishing compound are detected in the

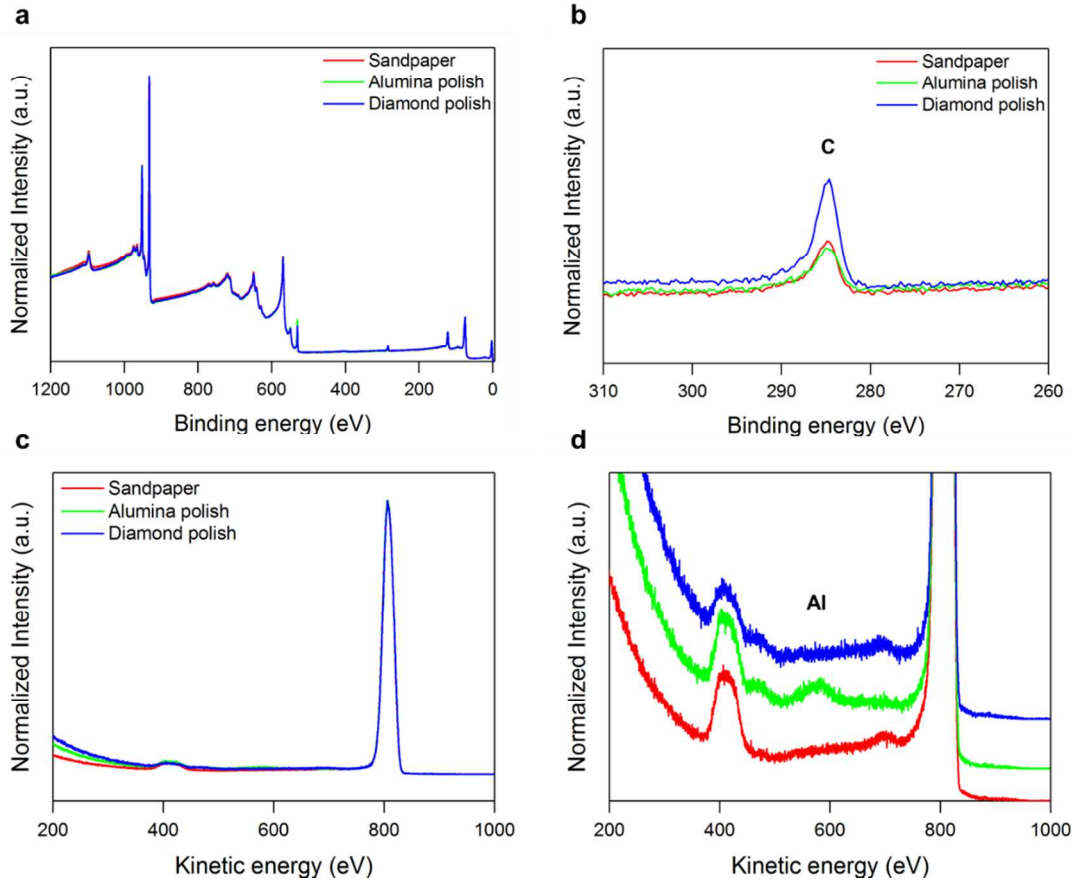

electrode surface after rising. This is especially problematic for alumina polishes as Al is an active HER metal.

Figure S3: Surface characterization after different mechanical polishing pretreatments. a) XPS survey scan and b) C 1s scan for Cu foil prepared using three different pretreatments: sandpaper polishing, and mechanical polishing using an alumina and diamond slurry. Higher

carbon content is observed in the sample polished using diamond. c,d) Corresponding LEIS data. Aluminum is observed on the surface for the alumina polished sample.

SI-4: Quantification of the Hydrodynamic Boundary Layer Thickness

The hydrodynamic boundary layer thickness of an electrochemical cell can be quantified by measuring the diffusion-limited current of ferricyanide reduction:

$$Fe(CN)_6^{3-} + e^- \rightarrow Fe(CN)_6^{4-}$$

Ferricyanide reduction is an ideal reaction to probe the hydrodynamic boundary layer thickness due to its electrochemical reversibility, meaning that the reduction of ferricyanide is facile such that the observed rate is limited only by mass transfer regardless of the applied overpotential. When conducting this measurement, the total ferricyanide concentration should be minimized and the supporting electrolyte should be identical to that typically employed during CO_2 reduction. This will ensure that the fluid properties of the solution utilized to quantify the hydrodynamic boundary layer thickness accurately reflect those of the electrolytes typically employed to measure electrocatalytic activity. Furthermore, Au electrodes should be utilized to conduct the measurement to avoid Galvanic corrosion processes in which ferricyanide is the oxidizing agent. Figure S4A depicts cyclic voltammograms measured in 0.1 M $CsHCO_3$ electrolytes with and without the addition of 10 mM $K_3Fe(CN)_6$. There is a potential window of ~600 mV where the observed Faradaic current can be attributed entirely to ferricyanide reduction. Furthermore, the observed rate of ferricyanide reduction is independent of the applied voltage, which is a result of its electrochemical reversibility, as previously mentioned. Thus, the steady state diffusion-limited current density associated with ferricyanide reduction can be measured and utilized to calculate the average hydrodynamic boundary layer thickness at the cathode surface using Fick's law:

$$\delta_{BL} = \frac{F \times D_{Fe(CN)_6{}^{3-}} \times C^*_{Fe(CN)_6{}^{3-}}}{J_{SS}}$$

As shown in Figure S4B, the steady state current density associated with ferricyanide reduction increases as the flow rate of CO_2 through the cell increases, which occurs due to the enhanced mixing of the electrolyte by the column of CO_2 bubbles near the cathode.

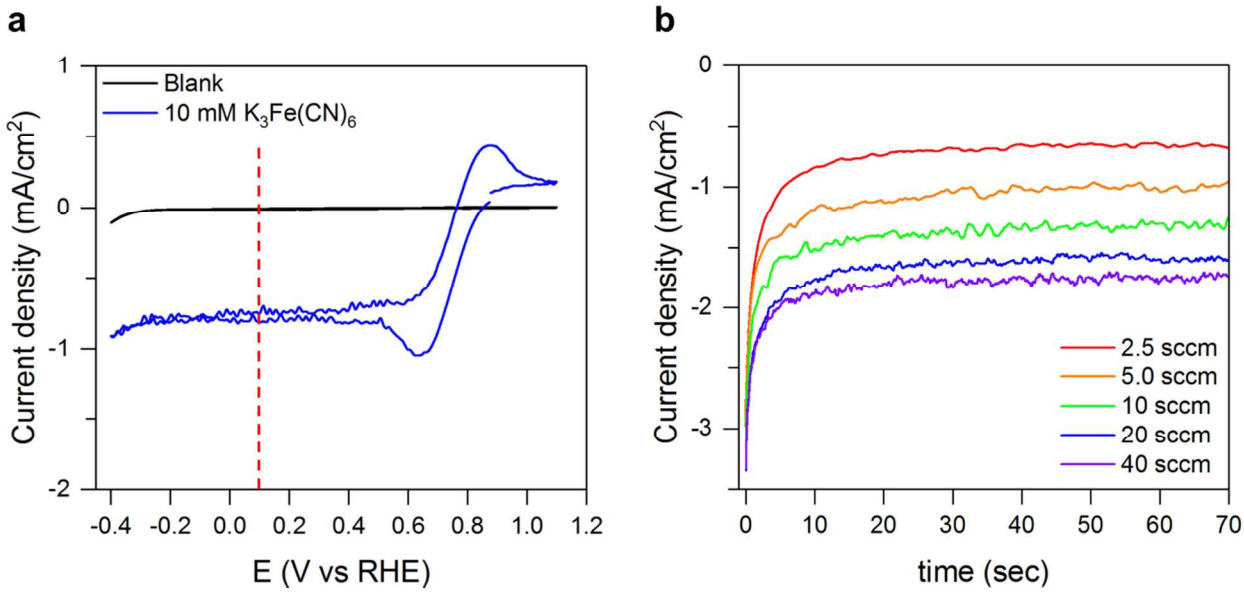

Figure S4: Quantification of the hydrodynamic boundary layer thickness of an electrochemical cell. a) Cyclic voltammograms obtained in 0.1 M $CsHCO_3$ saturated with CO_2 with and without the addition of 10 mM $K_3Fe(CN)_6$. The dotted red line indicates the potential used in the subsequent chronoamperometry experiments. b) Chronoamperometry experiments utilized to measure the diffusion-limited current density of ferricyanide reduction under a series of different hydrodynamic conditions.

SI-5: XPS and LEIS Analysis of Tested Polycrystalline Ag Films

XPS and LEIS were conducted on the polycrystalline Ag thin films tested under different hydrodynamic conditions to confirm that the observed trends were not being influenced by varying impurity concentrations. As shown in Figure S5, all electrodes were observed to be completely free of contamination within the detection limits of XPS and LEIS.

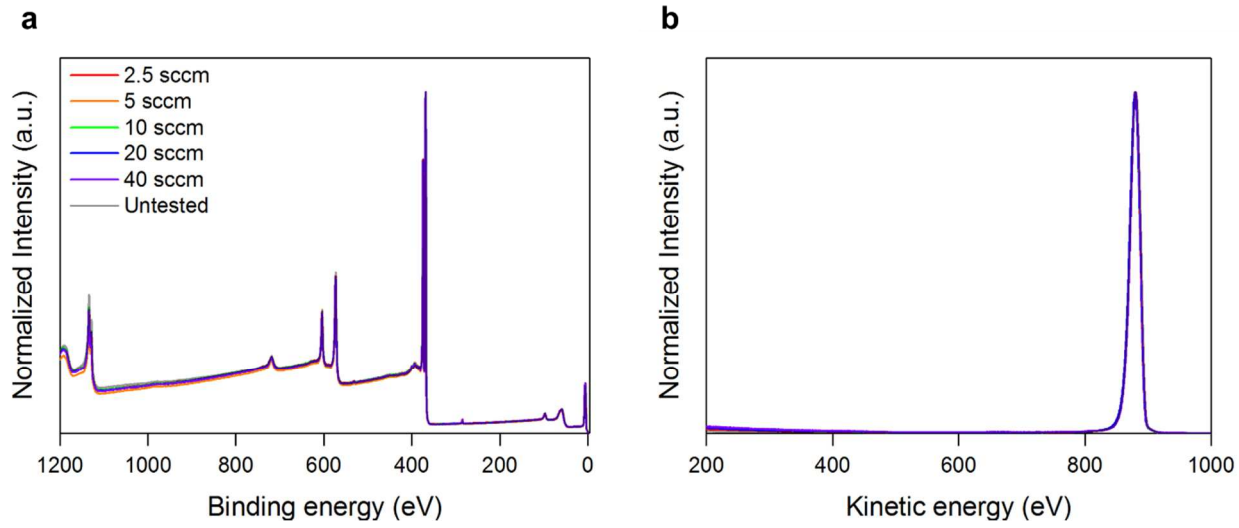

Figure S5: Spectroscopic characterization of the surface of polycrystalline Ag before and after chronoamperometry staircases in Chelex-pretreated 0.1 M $CsHCO_3$ using a glassy carbon anode. a) XPS and b) LEIS.

SI-6: Dependence of the Measured Activity of Polycrystalline Ag on the Hydrodynamics of the Electrochemical Cell

The CO partial current density observed over polycrystalline Ag deviates from Tafel kinetics at roughly -1 V vs RHE, as shown in Figure S6. This deviation is due to concentration polarization of the electrode surface. As a result, the observed activity at potentials negative of -1 V vs RHE is dependent on the hydrodynamics of the electrochemical cell. To illustrate this the maximum rate of CO_2 consumption over polycrystalline Ag was measured under a series of different hydrodynamic conditions. The maximum rate of CO_2 consumption was found to scale inversely with the hydrodynamic boundary layer thickness, as shown on Figure S7. This is exactly what would be expected for a reaction that is limited by diffusive mass transfer of a reactant through a stagnant boundary layer.

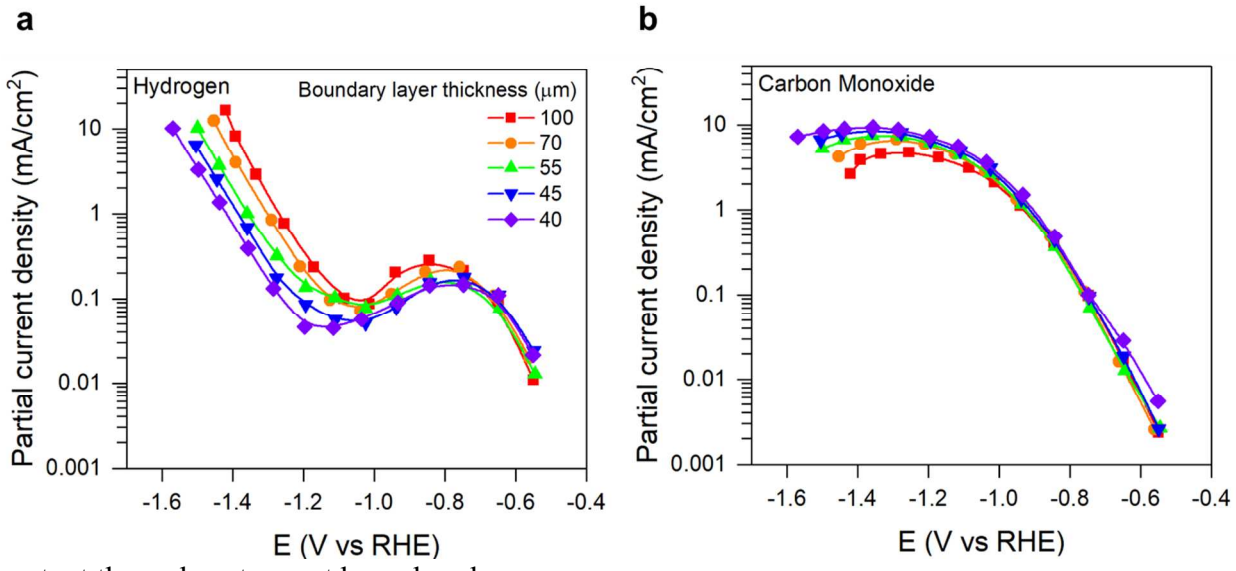

Figure S6: Dependence of the measured activity of polycrystalline Ag on the hydrodynamics of the electrochemical cell. a) H_2 partial current density. b) CO partial current density.

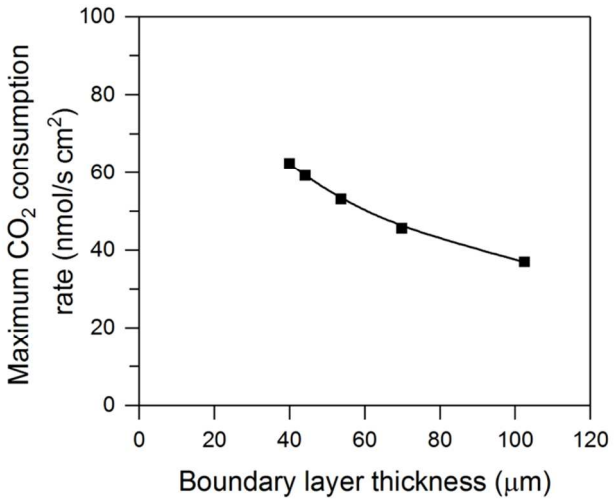

Figure S7: Maximum rate of CO_2 consumption observed over polycrystalline Ag in 0.1 M $CsHCO_3$ under different hydrodynamic regimes.

SI-7: Calculation of the Significance of Electrolyte Impurities

The concentration of contaminants in the catholyte that result in a coverage of 0.1 ML equivalents on the cathode surface was calculated assuming a surface atom density of 10^{15} atoms/cm^2 and that all the impurities in the electrolyte are deposited onto the cathode surface over the course of electrolysis using:

$$C = \frac{A/V * RF}{6.022}$$

Where:

C	Concentration of impurities resulting in 0.1 ML coverage
A	Geometric surface area of cathode
V	Catholyte volume
RF	Roughness factor of the cathode

SI-8: Quantification of Surface Roughness by Capacitive Cycling

The surface roughness of the electrochemically cycled Ag electrode was determined relative to a mechanically polished Ag foil by taking the ratio of their double layer capacitances. The double layer capacitance was determined by measuring the charging current in a potential range where no Faradaic processes occur at a series of increasingly rapid scan rates, as shown in Figure S8a. The double layer capacitance was then determined by calculating the scan rate dependence of the observed charging current, as shown in Figure S8b. Finally, the roughness factor of the electrochemically cycled electrode was determined by normalizing the calculated double layer capacitance by that measured over the mechanically polished Ag foil.

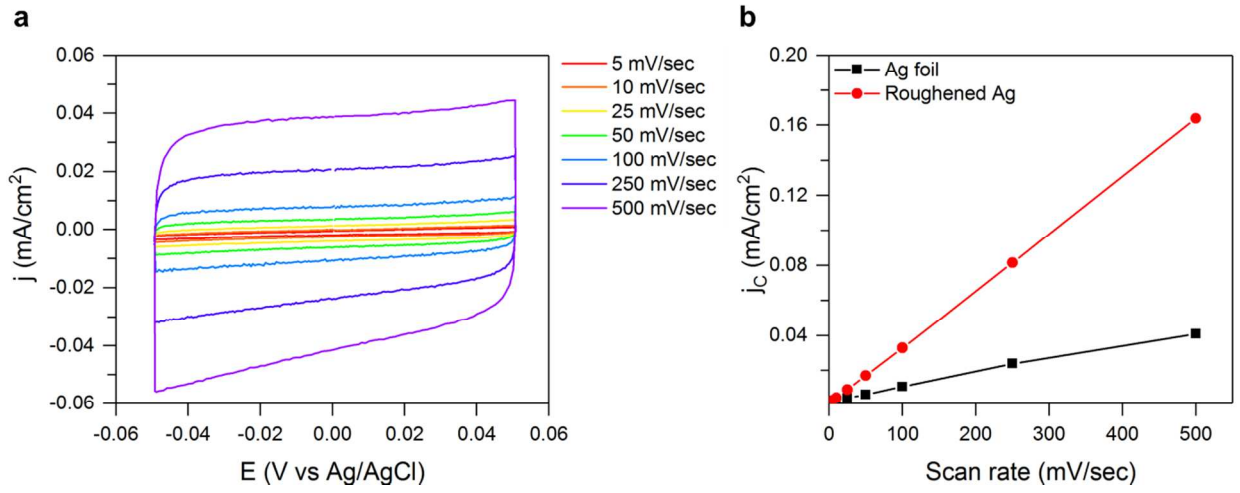

Figure S8: Determination of relative roughness of Ag catalysts a) Capacitive cycling of a mechanically polished Ag foil over a 100 mV non-Faradaic region in a 0.1 M $HClO_4$ electrolyte. b) Capacitive current vs scan rate.

SI-8: Comparison of ECSA Normalized Activity of Cu-Based Catalysts

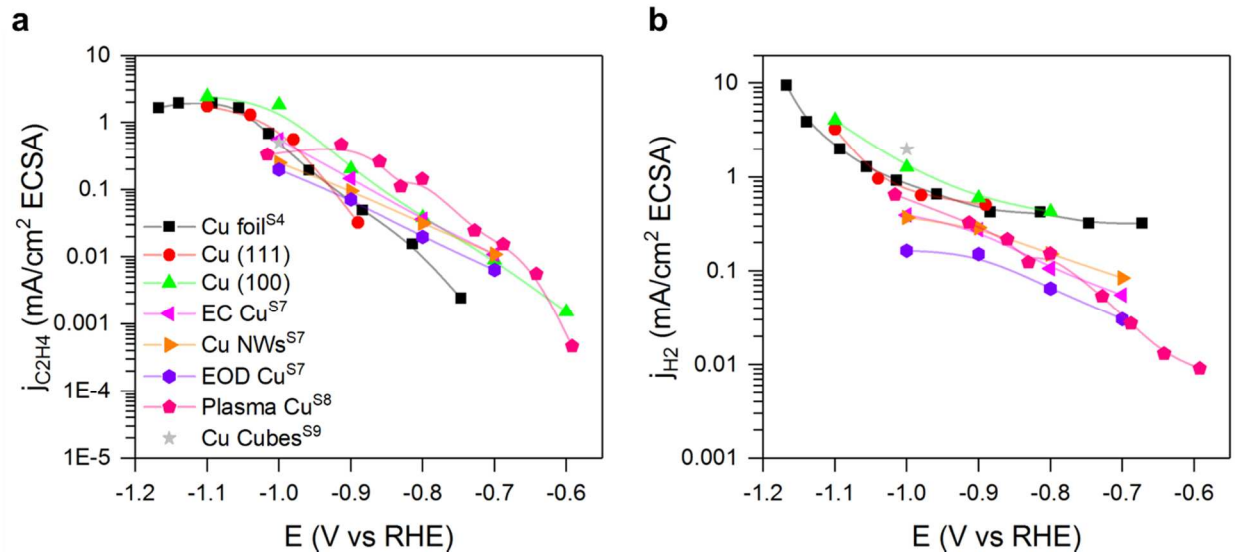

Figure S9: Comparison of ECSA normalized activity of different Cu catalysts. Surface area normalized partial currents for a) ethylene and b) hydrogen over a variety of Cu-based catalysts.

References

1. Lobaccaro, P.; Singh, M. R.; Clark, E. L.; Kwon, Y.; Bell, A. T.; Ager, J. W. Effects of Temperature and Gas-Liquid Mass Transfer on the Operation of Small Electrochemical Cells for the Quantitative Evaluation of CO_2 Reduction Electrocatalysts. *Phys. Chem. Chem. Phys.* **2016,** 18, 26777-26785.

2. Hatsukade, T.; Kuhl, K. P.; Cave, E. R.; Abram, D. N.; Jaramillo, T. F. Insights into the Electrocatalytic Reduction of CO_2 on Metallic Silver Surfaces. *Phys. Chem. Chem. Phys.* **2014,** 16, 13814-13819.

3. Hahn, C.; Hatsukade, T.; Kim, Y.-G.; Vailionis, A.; Baricuatro, J. H.; Higgins, D. C.; Nitopi, S. A.; Soriaga, M. P.; Jaramillo, T. F. Engineering Cu Surfaces for the Electrocatalytic Conversion of CO_2: Controlling Selectivity toward Oxygenates and Hydrocarbons. *Proc. Natl. Acad. Sci.* **2017,** 114, 5918-5923.

4. Kuhl, K. P.; Cave, E. R.; Abram, D. N.; Jaramillo, T. F. New Insights into the Electrochemical Reduction of Carbon Dioxide on Metallic Copper Surfaces. *Energy Environ. Sci.* **2012,** 5, 7050-7059.

5. Tang, W.; Peterson, A.; Varela, A.; Jovanov, Z.; Bech, L.; Durand, W.; Dahl, S.; Norskov, J.; Chorkendorff, I. The Importance of Surface Morphology in Controlling the Selectivity of Polycrystalline Copper for CO_2 Electroreduction. *Phys. Chem. Chem. Phys.* **2012,** 14, 76-81.

6. Terunuma, Y.; Saitoh, A.; Momose, Y. Relationship Between Hydrocarbon Production in the Electrochemical Reduction of CO_2 and the Characteristics of the Cu Electrode. *J. Electroanal. Chem.* **1997,** 434, 69-75.

7. Lum, Y.; Yue, B.; Lobaccaro, P.; Bell, A.T.; Ager, J. W.; Optimizing C–C Coupling on Oxide-Derived Copper Catalysts for Electrochemical CO_2 Reduction. *J. Phys. Chem. C.* **2017,** *121,* 14191-14203.

8. Mistry, H.; Varela, A. S.; Bonifacio, C. S.; Zegkinoglou, I.; Sinev, I.; Choi, Y. W.; Kisslinger, K.; Stach, E. A.; Yang, J. C.; Strasser, P.; Cuenya, B. R. Highly Selective Plasma-Activated Copper Catalysts for Carbon Dioxide Reduction to Ethylene. *Nat. Commun.* **2016,** 7, 1-9.

9. Roberts, F. S.; Kuhl, K. P.; Nilsson, A. Electroreduction of Carbon Monoxide over a Copper Nanocube Catalyst: Surface Structure and pH Dependence on Selectivity. *ChemCatChem* **2016,** 8, 1119-1124.